Blue Light-Emitting Diodes with Good Spectral Stability Based on Blends of Poly(9,9-dioctylfluorene): Interplay between Morphology, Photophysics, and Device Performance

Abhishek P. Kulkarni and Samson A. Jenekhe*

Department of Chemical Engineering and Department of Chemistry, University of Washington, Seattle, Washington 98195-1750

Received April 13, 2003; Revised Manuscript Received May 9, 2003

ABSTRACT: Spectrally stable blue electroluminescence (EL) is obtained from single-layer polymer light-emitting diodes fabricated from binary blends of conjugated poly(9,9-dioctylfluorene) (PFO) with either thermally stable poly(vinyl diphenylquinoline) (PVQ) or polystyrene. The brightness and EL efficiency of the polymer blend LEDs were enhanced by a factor of 5−14 compared to the PFO homopolymer devices. The additional green emission observed in the EL spectra of pure PFO devices was substantially suppressed in the blend LEDs. The electrical characteristics of the diodes and electric-field-modulated PL spectroscopy results indicate increased spatial confinement induced exciton stability and electron−hole recombination efficiency in the blend devices. The variation of the device performance with blend composition is related to the phase-separated morphology of the blends. The origin of the spectral stability lies in the improved thermal stability of the PFO:PVQ blends due to the high glass transition temperature (T_g) of PVQ (185 °C). These results demonstrate that blending of PFO with high T_g charge transport or charge blocking polymers is a simple strategy to overcoming the problem of poor spectral stability of blue-emitting polyfluorenes.

Introduction

Organic light-emitting diodes based on conjugated polymers are being developed for commercial applications in the display technology market for thin, flat panel, full color displays.[1−3] Efficient electroluminescence of the three primary colors, red, green, and blue, is essential to achieve full color displays. Although these three colors have been demonstrated in organic light-emitting diodes (OLEDs),[1−3] only the red and green OLEDs seem to have attained sufficiently high efficiencies and lifetimes for commercial applications.[1] Many challenges remain for improvement in the blue spectral region in terms of efficiency, durability in air, and spectral stability (color purity).

Polyfluorenes have recently emerged as an attractive class of electroluminescent conjugated polymers for blue LEDs due to their high photoluminescence quantum yields in the solid state (ca. 50%) and good charge transport properties.[3,4] One of the major current challenges in developing the polyfluorenes for blue LEDs is the poor spectral stability under normal operation with a broad EL band centered at 530−540 nm evolving with passage of current.[3] As a result, the pure blue emission changes to an undesired blue-green color. This band has been generally attributed to the formation of aggregates and/or interchain excimers in the polyfluorene films, and more recently to emissive keto defect sites produced due to thermo- or electro-oxidative degradation of the polyfluorene backbone.[5] Various approaches have been tried in an attempt to minimize or eliminate this undesirable long-wavelength emission band in polyfluorene-based LEDs.[6,7] The majority of these approaches have focused on chemical modifications of the polyfluorene main chain, including bulky side groups or end-capping groups.[6] Physical blends of low molecular weight hole-transporting molecules with a polyfluorene copolymer have also been explored to enhance emission in the blue with simultaneous suppression of excimer emission.[7a] However, many issues are yet unresolved about the troublesome excimer emission in blue emitting polyfluorenes and in achieving stable and efficient blue polyfluorene LEDs with good spectral stability.

Chart 1

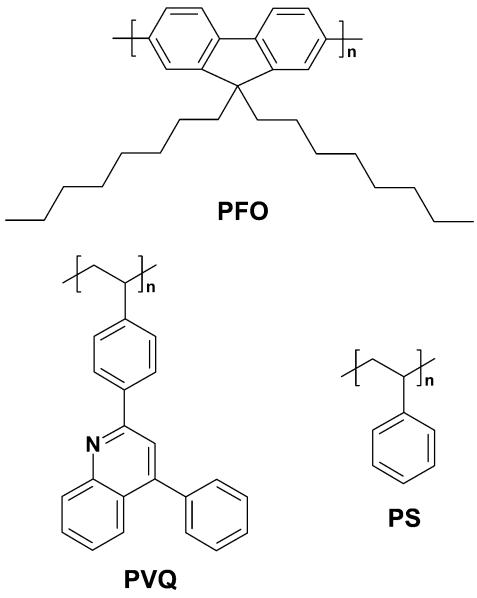

In this paper, we report single-layer blue LEDs with improved spectral stability and enhanced device performance from binary blends of poly(9,9-dioctylfluorene) (PFO) and a nonconjugated polymer, poly(vinyl diphenylquinoline) (PVQ) or polystyrene. The molecular structures of the polymers used in this study are shown in Chart 1. The photophysics of the PFO blends was investigated by optical absorption, steady-state photoluminescence (PL), and electric-field-modulated PL

* To whom correspondence should be sent. E-mail: jenekhe@cheme.washington.edu.

10.1021/ma0344700 CCC: $25.00 © 2003 American Chemical Society
Published on Web 06/20/2003

spectroscopy. The morphology of the blends was characterized by tapping mode atomic force microscopy (AFM) and fluorescence optical microscopy. The performance of the blend LEDs as a function of blend composition was correlated to the phase-separated morphology of the blends.

Experimental Section

Materials. The detailed synthesis, characterization, and solution and thin film photophysical properties of poly(vinyl diphenylquinoline) (PVQ) were previously reported by our group.[8] The PVQ sample has a polydispersity of 1.09 and a molecular weight (M_w) of 93 000. Poly(9,9-dioctylfluorene) (PFO) and polystyrene (PS) were purchased from American Dye Source, Inc., and Polysciences with M_w of 10 000 and 100 000, respectively. High purity HPLC grade chloroform from Fisher Scientific was used as received for making solutions of homopolymers and binary blends.

Preparation of Blends and Thin Films. Binary blends of PFO with both PVQ and PS were made by mixing appropriate volumes of 0.5−0.7 wt % homopolymer solutions in chloroform. Compositions of blends in this report refer to weight percentage (wt %) of PVQ or PS. A series of 10−11 blend compositions were prepared in each case.

Thin films for optical absorption and PL measurements were spin-coated on glass slides. All the films were dried at 60 °C typically overnight in a vacuum to remove any residual solvent. Blend films (50−60 nm thick) were homogeneous and showed good optical transparency. For heat treatment studies, thus dried blend films were further annealed at 100, 150, and 200 °C in air or vacuum for a period of 2 h, cooled to room temperature, and investigated under ambient conditions.

Optical Absorption and Photoluminescence Spectroscopy. Optical absorption spectra were recorded using a Perkin-Elmer model Lambda 900 UV/vis/near-IR spectrophotometer. Steady-state PL studies were done on a Photon Technology International (PTI) Inc. model QM-2001−4 spectrofluorimeter.

Morphology. The thin film morphology of the homopolymers and their blends was characterized by atomic force microscopy (AFM) using a Nanoscope III microscope (Digital Instruments, Santa Barbara, CA) in standard tapping mode. Since standard tapping mode AFM is not chemically specific, fluorescence optical microscopy using a Leica DMIRB inverted fluorescence microscope was carried out to investigate further the morphology of the blends and assign the phases unambiguously. In blends of PFO with PS, an excellent contrast could be observed which helped in clear identification of the component phases.

Fabrication and Characterization of LEDs. The single-layer LEDs were fabricated as sandwich structures between aluminum (Al) cathodes and indium−tin oxide (ITO) anodes. ITO-coated glass substrates (Delta Technologies Ltd., Stillwater, MN) were cleaned sequentially in ultrasonic bathes of detergent, 2-propanol/deionized water (1:1 volume) mixture, toluene, deionized water and acetone. A 50 nm thick hole injection layer of poly(ethylenedioxythiophene) doped with poly(styrenesulfonate) (PEDOT:PSS) was spin-coated on top of ITO from a 1.3 wt % dispersion in water and dried at 200 °C for 1.5 h under vacuum. Thin films of PFO and its blends with PVQ or PS were spin-coated from their chloroform solutions onto the PEDOT layer and dried at 60 °C in a vacuum overnight. The film thicknesses obtained were 50−60 nm, which were measured by an Alpha-Step 500 surface profiler (KLA Tencor, Mountain View, CA). Finally, 100−120 nm Al electrodes were thermally evaporated through a shadow mask onto the polymer films. The equipment used was an AUTO 306 vacuum coater (BOC Edwards, Wilmington, MA) and typical evaporations were carried out at base pressures lower than 2×10^{-6} Torr. The area of each EL device was 0.2 cm^2. Electroluminescence (EL) spectra were obtained using a PTI QM-2001−4 spectrophotometer. Current−voltage characteristics of the LEDs were measured using a HP4155A semiconductor parameter analyzer (Yokogawa Hewlett-Packard, Tokyo). The luminance was simultaneously measured using a model 370 optometer (UDT instruments, Baltimore, MD) equipped with a calibrated luminance sensor head (model 211). The device external quantum efficiencies were calculated using a standard expression involving the measured ratio of forward directed luminance and device current density, taking into account the EL spectral distribution and the photopic spectrum.[9] All the device fabrication and characterization steps were done under ambient laboratory conditions.

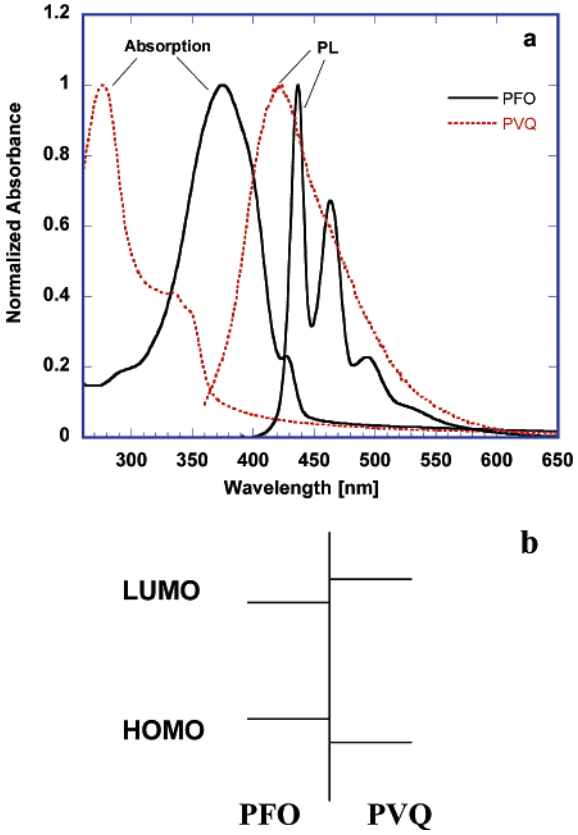

Figure 1. (a) Optical absorption and PL spectra of thin films of PFO and PVQ. The excitation wavelength for PFO was 380 nm and that for PVQ was 335 nm. (b) Schematic of the HOMO − LUMO energy levels in the PFO:PVQ blend system.

Electric-Field-Modulated Photoluminescence Spectroscopy. Electric-field-modulated PL studies were done on the same devices after their EL properties had been characterized. An LED sample is photoexcited, and the PL emission spectrum is acquired under an applied bias voltage. Both forward and reverse bias voltages gave identical PL spectra before the onset of EL emission. All the experimental conditions were similar to the steady-state PL measurements.

Results and Discussion

Electronic Structure and Properties of Homopolymers. Figure 1a shows the optical absorption and PL spectra of thin films of PFO and PVQ homopolymers. A broad featureless absorption peak at 380 nm is seen along with a narrower, well-resolved peak at 433 nm superimposed on the bulk absorption of PFO films. The optical band gap of PFO from the absorption edge is 2.95 eV. The highest occupied molecular orbital (HOMO) and lowest unoccupied molecular orbital (LUMO) energy levels of PFO have been reported in the literature to be in the ranges 5.6−5.8 and 2.12−2.6 eV, respectively.[10] PVQ has a broad PL spectrum with emission maxima at 420 nm. The structured PFO emission in the solid state has peaks at 436, 463, and 494 nm. The PL emission spectrum of PFO in nonpolar

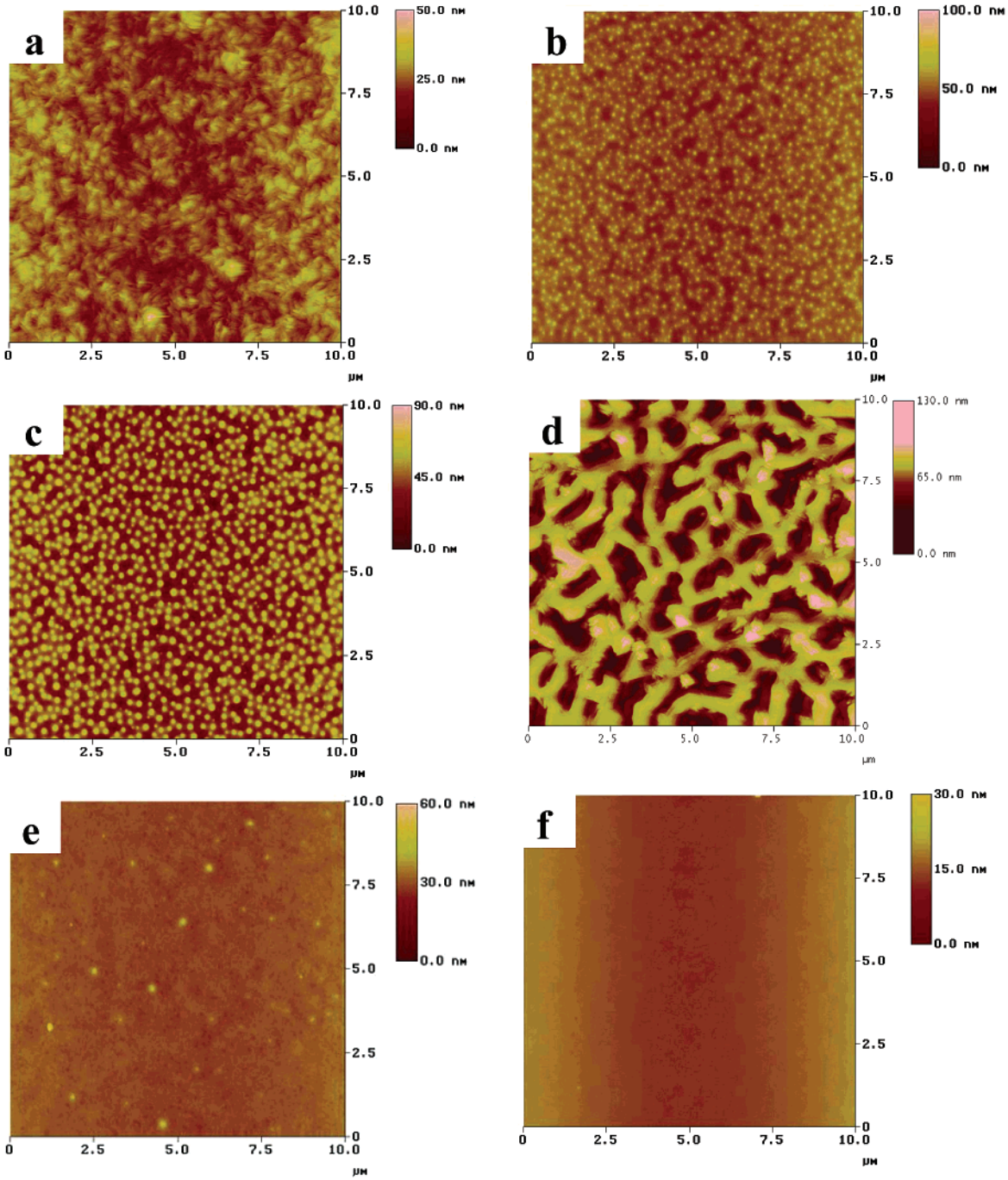

Figure 2. AFM topographic images (10 × 10 μm) of PFO:PVQ blend system: (a) PFO, (b) 5%, (c) 20%, (d) 40%, (e) 70% PVQ, and (f) PVQ. Films were spin-coated on silicon, dried at 60 °C in a vacuum and imaged at room temperature.

solvents (not shown) shows a well-resolved structure with peaks at 420, 448, and 472 nm assigned to singlet intrachain excitons.[11] There is a red-shift of the peaks by 15−20 nm in going from the dilute solution to the thin film, a fact that is reported in the literature and attributed to aggregate emission in the solid state.[11]

PFO has a rich temperature-dependent phase behavior, with a glass transition temperature at $T_g \sim 75$ °C and a liquid crystal (LC) phase transition at $T_{LC} \sim 160$ °C above which it becomes a birefringent fluid.[11a,b] PVQ forms colorless films on glass with an absorption onset at 360 nm, giving an optical band gap of 3.45 eV. It is a thermally stable polymer with a $T_g \sim 185$ °C.[8] Unlike conjugated polyquinolines,[12] which have relatively small band gaps (<3 eV) and high electron affinities (ca. 2.5 − 3.0 eV), that show good electron transport properties, PVQ is not expected to improve electron transport in the blends. Figure 1b shows a schematic of the relative HOMO−LUMO energy levels in the PFO:PVQ blends which are important to understanding the photophysical and charge trapping processes in the blends.

Morphology of PFO Blends. When two homopolymers are blended together in solution and spun-cast into thin films, phase separation is to be expected due to the low entropy of mixing for long polymer chains and the chemical incompatibility between the components.[13] The morphology of conjugated polymer blends is known to affect the device performance in polymer blend devices such as LEDs, solar cells, and thin-film transistors.[14] We thus investigated the morphology of the PFO blends with standard tapping mode AFM and fluorescence optical microscopy.

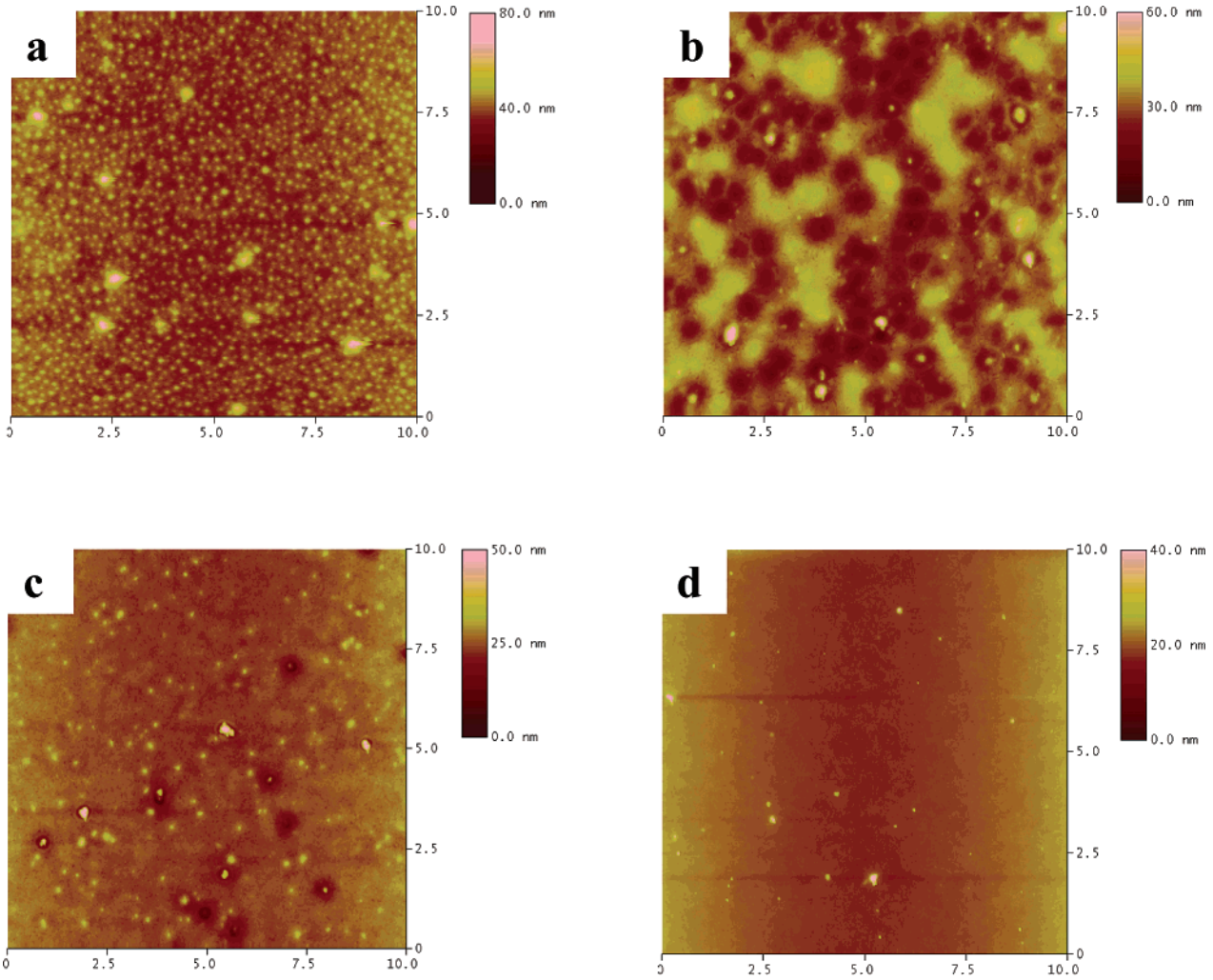

Figure 3. AFM topographic images (10 × 10 μm) of PFO:PS blends: (a) 10%, (b) 30%, (c) 50%, and (d) 90% PS. Films were spin-coated on silicon, dried at 60 °C in a vacuum, and imaged at room temperature.

Figure 2 shows the topographic AFM images of PFO, PVQ, and their blends. Figure 2a shows the pure PFO film morphology, revealing a structured topography and thus indicating the presence of clusters or aggregates with some alignment within the clusters. The AFM images of Figure 2, parts b−e correspond to 5, 20, 40, and 70% PVQ blends. A clear phase separation on the length scale of 100−500 nm can be seen. In the 3−30% PVQ blends, 20−40 nm tall isolated domains, nearly spherical and monodisperse in size are observed; these phase-separated morphologies are of the nucleation and growth type. The corresponding phase images (not shown) indicated that the raised morphological features did not possess any fine structure, suggesting that they probably correspond to a single polymer phase. For the 40% PVQ blend, the topographic image shows an interconnected network morphology reminiscent of spinodal decomposition (Figure 2d). Beyond 50% PVQ, the number of the raised features or phase-separated domains decreases and the topography smoothens gradually, giving a featureless film for the pure PVQ as seen in Figure 2f. Using fluorescence optical microscopy, it was found that the raised features showed a much higher contrast for blue emission. Thus, we can assign them to the PFO polymer phase as PFO has a much higher PL quantum yield compared to PVQ.

The phase separated morphology of PFO:PS blends (Figure 3) was found to be quite similar to PFO:PVQ blends. In the case of the 10% PS blend (Figure 3a), we see the formation of spherical domains throughout the film similar to the 5% PVQ blend (Figure 2b). The number of domains seen in the AFM height image decreased with increasing polystyrene content in the blend. This can be clearly seen in going from the 50% blend (Figure 3c) to the 90% blend (Figure 3d). The similarity in morphology between the PFO:PVQ and PFO:PS blends dried at 60 °C leads to comparable device performance with blend composition as discussed later.

The similarity in morphologies seen for both PFO blends occurred only when the films were dried at 60 °C, which is below the T_g of both components. However, on annealing the blends at higher temperatures, the morphology varied significantly between the PVQ and PS blends. When the PFO:PS blends were annealed at 100 °C, which is close to the T_g of polystyrene, in air or vacuum, perfectly spherical domains with diameters of 2−15 μm were observed as exemplified in Figure 4 for the 50% blend. These large-diameter spherical domains in the phase-separated blends after annealing at high temperatures are to be contrasted with 200-nm domains resulting from low temperature (60 °C) annealing. The fluorescence optical micrographs confirmed that the spherical domains were the PFO phase. After annealing in a vacuum, the PL emission is blue (Figure 4a) whereas after annealing in air for the same time green

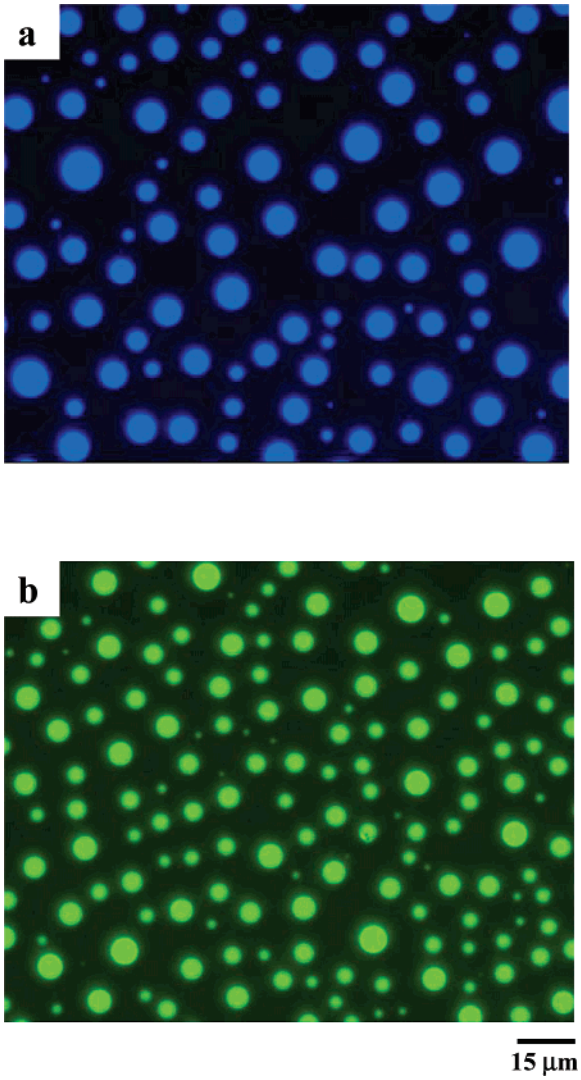

Figure 4. Fluorescence optical micrographs of 50% PFO:PS blends annealed at 100 °C in a vacuum (a) and in air (b).

PL (Figure 4b) is observed from the same blend film. This observation may be consistent with the claim that fluorenone defect sites formed by oxidation of fluorene in an oxygen-rich atmosphere are responsible for the undesirable green emission.[5b] However, whereas there is clear evidence that fluorenone defects are present in the photo- or electro-oxidized polyfluorene films,[5b] it is not yet clear if the green (530 nm) emission is due to the monomer (single chain) state or excimer state of the fluorenone defects. Because 9-fluorenone is more planar than 9,9-dialkylfluorene, it may well be that fluorenone defect production enhances excimer formation and consequently the 530 nm emission band. Similar spherical domains of PFO were also formed in the PFO:PVQ blends when the blend films were annealed at 200 °C. Thus, annealing above the T_g of both blend components is essential to forming these spherical aggregates of PFO. Changes in the photophysics of these PFO blends upon annealing at different temperatures are discussed in the next section.

Photophysics of PFO Blends. Figure 5a shows the optical absorption spectra of thin films of PFO, PVQ, and their blends after annealing at 60 °C under vacuum. PFO absorption has a broad peak at 380 nm whereas PVQ absorption has a shoulder at 335 nm and a peak at 280 nm. The absorption spectra of the blends are

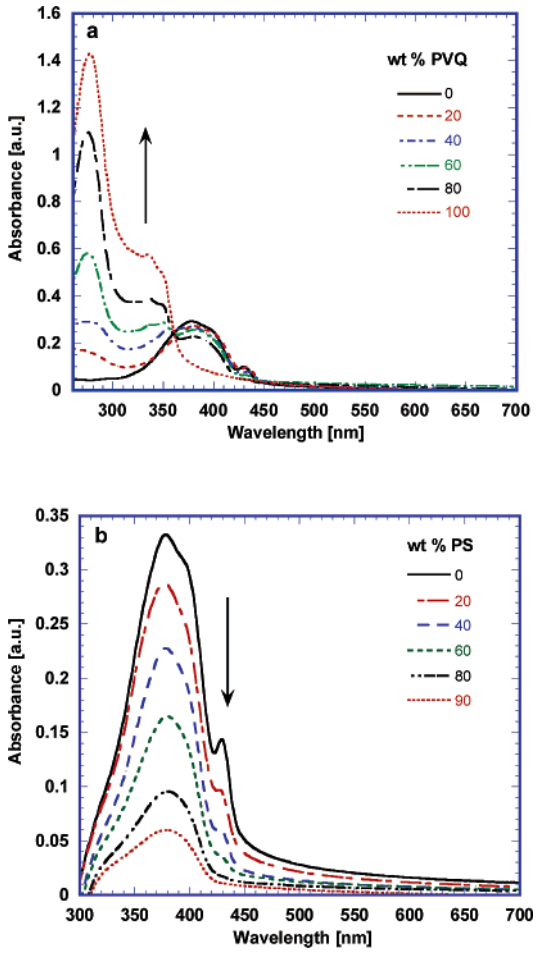

Figure 5. Optical absorption spectra of thin films dried at 60 °C in a vacuum: (a) PFO:PVQ blends and (b) PFO:PS blends.

superpositions of the homopolymer spectra indicating no ground-state interaction between the components. In Figure 5a, we find that an additional small peak at 433 nm is present in the spectrum of PFO film. This peak has been attributed to aggregates containing PFO chains that possess a more ordered intrachain conformation and hence a more delocalized ground-state electronic structure.[11c,d] In the PFO:PVQ blends, although the peak intensity decreases with increasing concentration of PVQ, even the 80% PVQ blend shows a modest peak at 433 nm. Similar results were obtained for PFO:PS blend films baked at 60 °C as shown in Figure 5b. After the blends were annealed at temperatures above the T_g of either blend component, this 433 nm aggregate peak disappears from the absorption spectra of all the blend compositions (not shown).

Figure 6a shows the normalized PL emission spectra of PFO:PVQ blend thin films dried at 60 °C. The emission predominantly is from PFO with a peak at 436 nm. A shoulder at 420 nm emerges and increases with increasing fraction of PVQ in the blends. All the blends from 3% to 80% PVQ have the dominant 436 nm PL emission due to PFO. Only in the 90% PVQ blend (not shown) is a PL maximum at 420 nm observed, and we note the absence of the aggregate peak at 433 nm in the absorption spectrum of this blend composition. To study the effect of the annealing temperature on the PL emission of PFO:PVQ blends, we annealed the blend films at 100, 150, and 200 °C in air for 2 h after the initial baking at 60 °C in a vacuum. Since our goal was

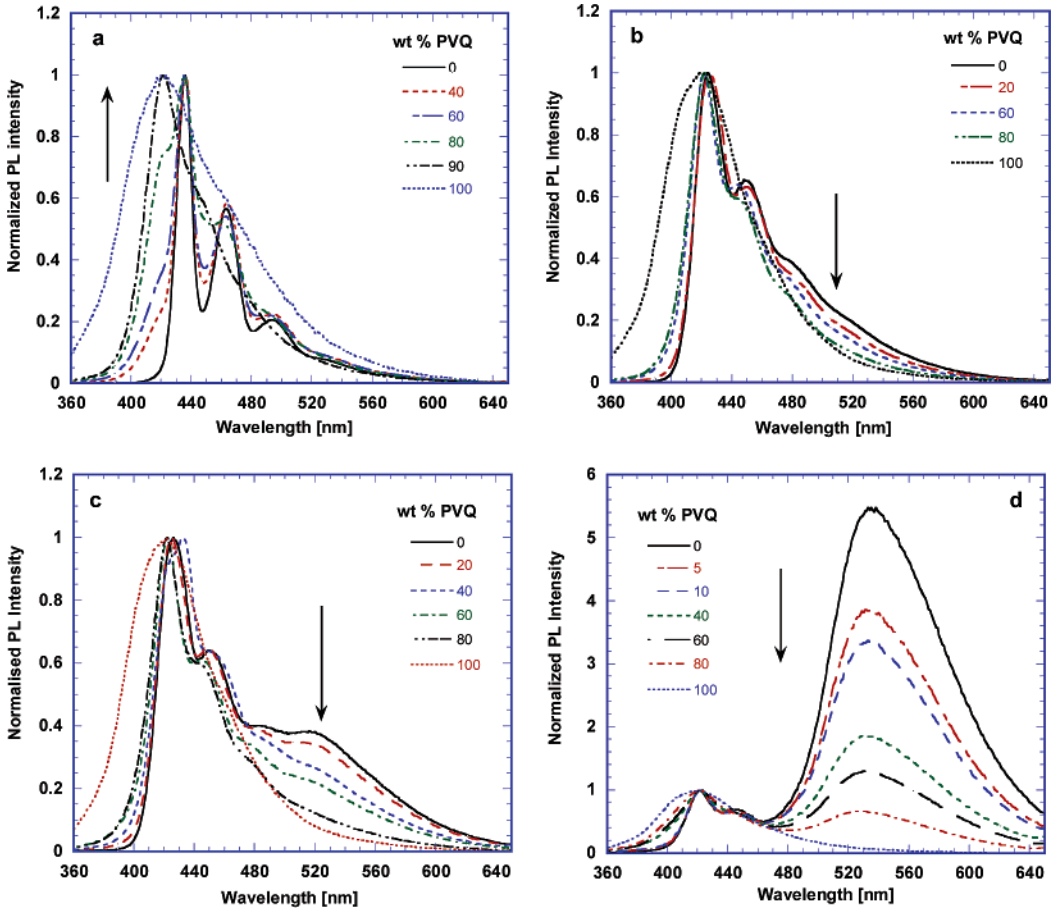

Figure 6. PL emission spectra (335 nm excitation) of thin films of PFO, PVQ, and their blends annealed at different temperatures in air for 2 h: (a) 60 °C (in a vacuum); (b) 100 °C; (c) 150 °C; (d) 200 °C.

to see whether the green excimer emission is suppressed in the blends, it was thought that such heating would simulate the heat developed in the blend EL devices under applied bias and help predict the spectral stability of the blue EL emission. Parts b−d of Figure 6 show the PL emission spectra of the blends annealed at 100, 150, and 200 °C, respectively. In all three cases, the dominant PL peak shifted from 436 to 420 nm in both pure PFO and the blends, with a simultaneous disappearance of the aggregate peak at 433 nm in their absorption spectra. For the blends annealed at 100 °C (lower than T_g of PVQ), there is no evidence of the green excimer emission at 530 nm (Figure 6b). In the case of blends annealed at 150 °C (Figure 6c), there is a slight increase in the excimer emission, with the relative intensity at 530 nm decreasing with increasing PVQ content in the blends. The most dramatic effect was observed for films annealed at 200 °C, which is greater than both the T_g of PVQ (185 °C) and PFO (75 °C). Figure 6d shows that the green emission at 530 nm is 5−6 times more intense than the blue emission at 420 nm for pure PFO. Such strong excimer[15] emission has been reported for different polyfluorenes after similar annealing treatments.[16]

Figure 7a shows the PL emission spectra of the PFO:PS blends dried at 60 °C. The shoulder peak at 420 nm increases in intensity with increasing dilution of PFO in the PS matrix. In the 90% PS blend, the PL emission peak maxima is at 420 nm, consistent with single chain emission from PFO which is now presumably molecularly dispersed in the PS matrix. Figure 7b shows the PL emission spectra of 50% PS blend after various heat treatments. Annealing at 200 °C in air instead of vacuum leads to a 6-fold increase in the green emission band. Nonetheless, it can be seen that the extent of excimer emission is suppressed monotonically with increasing PVQ fraction in the PFO:PVQ blends even on annealing in air (Figure 6d). We thus confirm spectroscopically that oxygen plays a key role in the formation of excimers in polyfluorenes, in addition to the fluorescence micrographs discussed previously. Also, it can be expected from these results that the EL emission from these blends will be relatively more stable due to the greater heat resistance of the blends than the pure PFO and reduced aggregation of PFO.

Electroluminescence of PFO Blends. Representative EL spectra of PFO and some of its blends with PVQ are shown in Figure 8. As seen from Figure 8a, the spectral shape of the emission from pure PFO broadens with bias voltage and is very different from the PL spectrum of PFO, which has a vibronic progression with peaks at 436, 463, and 494 nm. Although the EL emission maxima is at 436 nm, a loss of resolution in the 463 nm peak is seen with subsequent voltage sweeps and eventually this peak becomes equal in intensity to the 436 nm peak. Simultaneously, the 494 nm peak becomes broader and develops a tail down into the 550 nm region. These kind of broad EL spectra and poor spectral stability are well documented problems with blue-emitting polyfluorenes.[5,6]

The EL spectra of PFO:PVQ blend devices have much better stability (spectral purity defined by the highest % of emission occurring at 436 nm) as shown in Figure 8, parts b−d, for the 5%, 10%, and 20% PVQ blends,

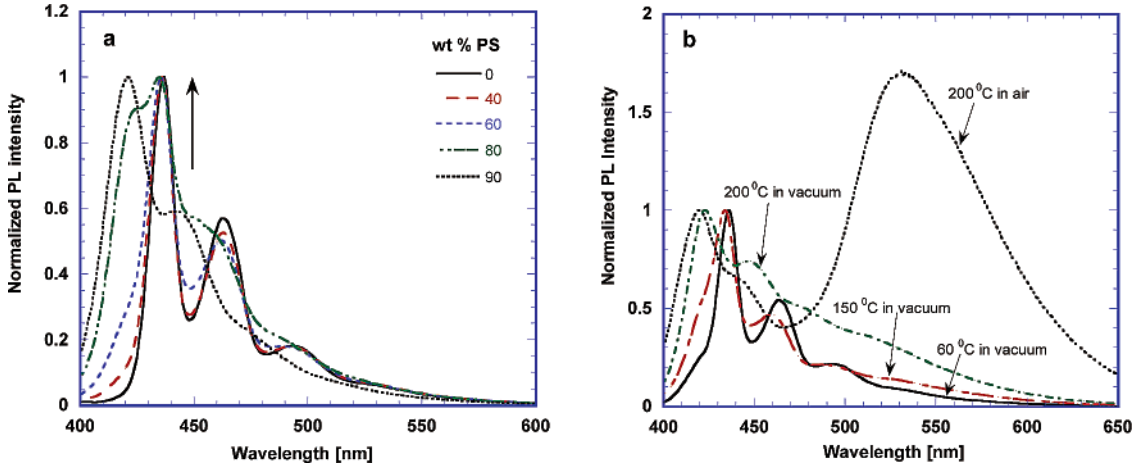

Figure 7. PL spectra of thin films of PFO:PS blends (a) dried at 60 °C in a vacuum and (b) 50 wt % blend with different heat treatments. The excitation wavelength was 380 nm in all cases.

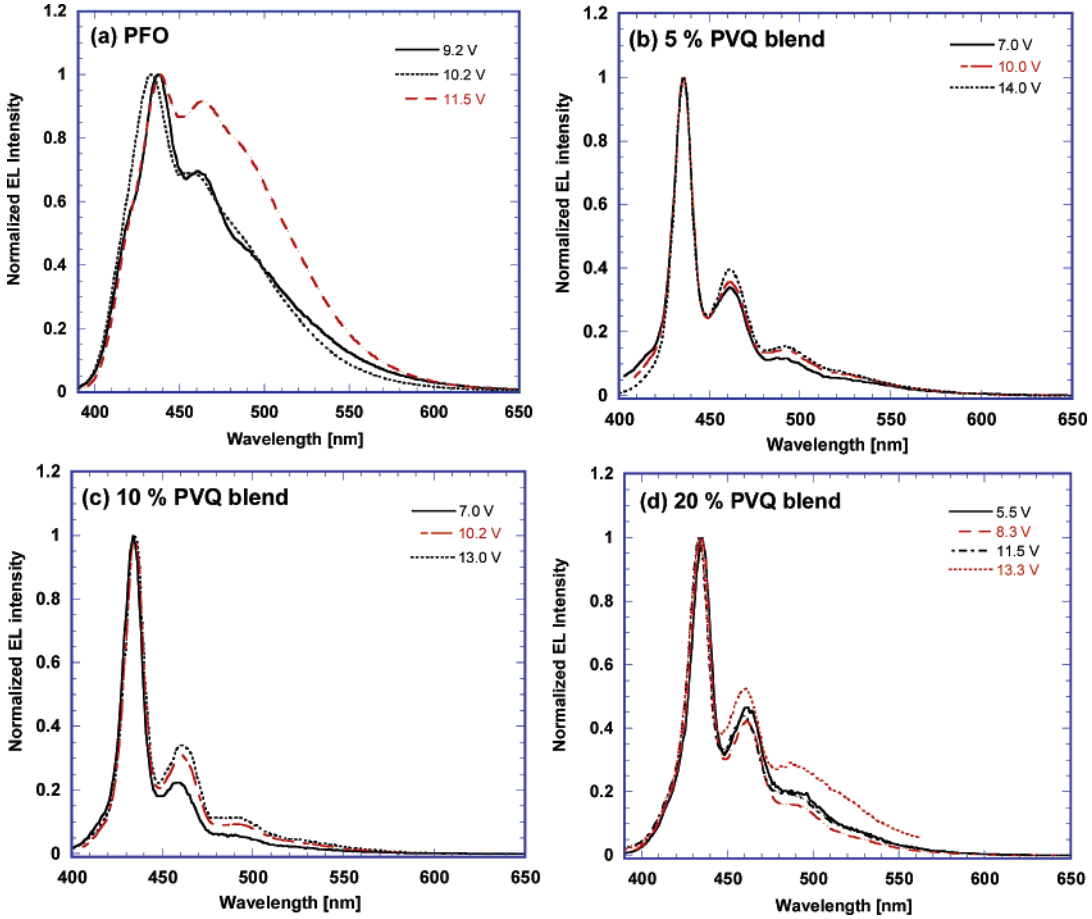

Figure 8. EL spectra of (a) PFO, (b) 5% blend, (c) 10% blend, and (d) 20% PVQ blend LEDs.

respectively. The peak at 436 nm is the dominant one with a good resolution in the 464 nm peak for voltage sweeps from the turn-on bias to the maximum bias for each diode. Although systematic device lifetime studies were not done, it should be pointed out that these EL spectra were reproducible for several sweeps on the same active pixel area. The broad green peak at 530 nm is also substantially suppressed in all the blend LEDs. Improved EL spectral stability was also observed in the PFO:PS blends as shown in Figure 9. The EL spectrum of the 5% PS blend LED is shown in Figure 9a, while the spectra of the 10% and 20% blends are shown in Figure 9, parts b and c. Although the EL spectral stability is better compared to the homopolymer PFO, we note that the blends with PVQ are relatively more stable than the PS blends. The peaks at 463 and 494 nm have a higher contribution to the overall EL spectra in the PS blends.

The current density−electric field and luminance−voltage characteristics of the PFO:PVQ blend LEDs are shown in Figure 10. The turn-on voltages of all the devices were around 5−6 V (∼(1−1.5) × 10^6 V/cm), with no significant variation with the blend composition. It was observed that beyond 50 wt % PVQ, there was no measurable luminance from the blend devices as the current levels were very low. No EL could be seen in pure PVQ devices which can be attributed to the very high band gap (3.45 eV) and the related large charge

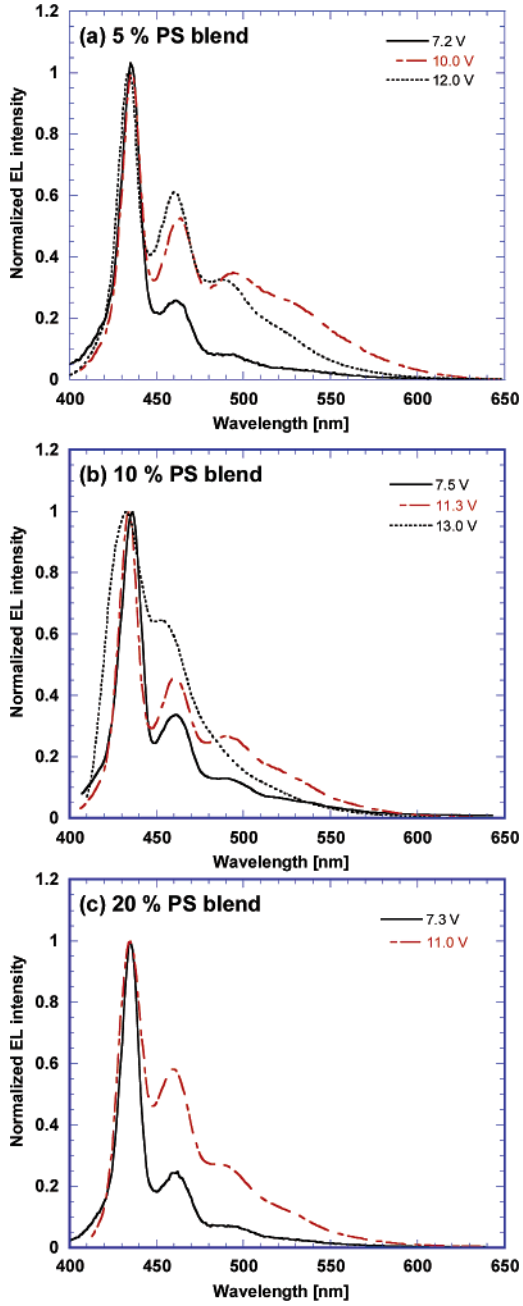

Figure 9. EL spectra of (a) 5% blend, (b) 10% blend, and (c) 20% PS blend LEDs.

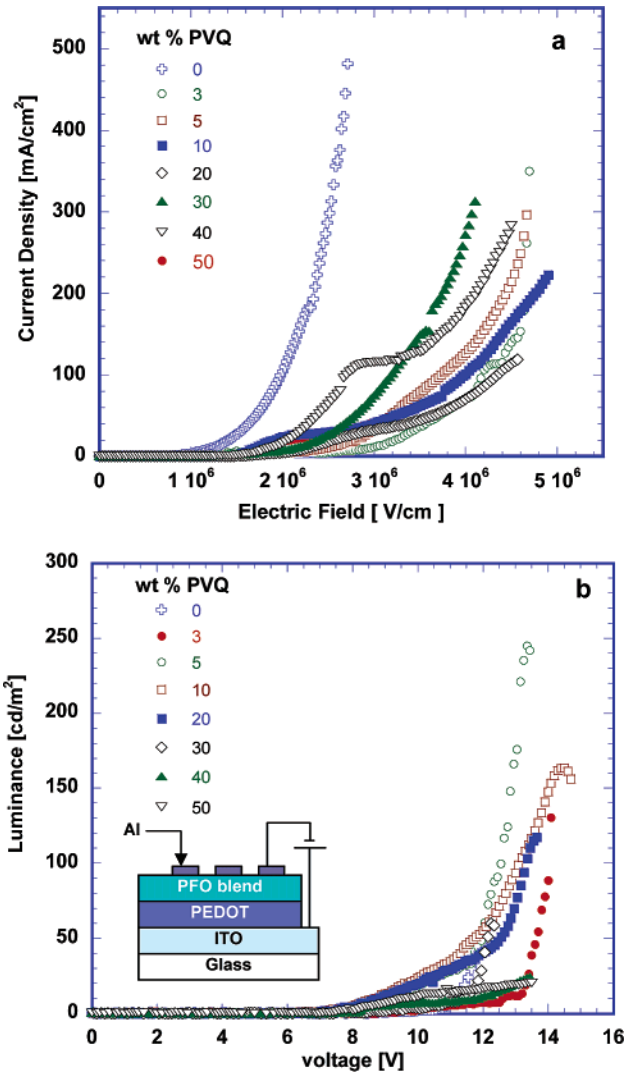

Figure 10. (a) Current density−electric field characteristics of LEDs: pure PFO and blends with PVQ. (b) Luminance−voltage characteristics of the devices in part a. The inset shows the device schematic.

injection barriers at both electrodes. The solid state fluorescence quantum efficiency of PVQ thin film is expected to be very low since the quantum efficiency in dichloromethane solution was only 7%.[8] Figure 10a shows that the currents passing through the blend devices are much lower than that through the pure PFO device for the same electric fields, suggesting that there is better charge recombination efficiency in the blends. The maximum brightness observed was 250 cd/m^2 at a bias of 14 V from the 5% PVQ blend (Figure 10b).

The device characteristics of the PFO:PS blend LEDs are shown in Figure 11. The trends in current density and luminance were similar to the PVQ blend devices. No detectable luminance was seen beyond 50 wt % PS due to problems with charge injection and the insulating nature of the PS matrix. Figure 11a shows that the currents through the blend LEDs are lower than that through the homopolymer device. The maximum luminance was 220 cd/m^2 at a bias of 13 V in the 10% PS blend (Figure 11b).

The brightness and EL external quantum efficiency as a function of blend composition are shown in Figure 12 for the PFO:PVQ blend LEDs. Figure 12a indicates that there is no measurable EL beyond 50 wt % PVQ. The pure PFO device has a maximum brightness of 60 cd/m^2 and a maximum EL efficiency of 0.01% at 11.5 V. Enhanced performance was found in the blends with a maximum brightness of 250 cd/m^2 and a maximum EL efficiency of 0.14% at 14 V for the 5% PVQ blend. Relative enhancement in terms of both brightness and efficiency was seen only in the 3−20 wt % PVQ blends. For the 30% PVQ blend, the performance is almost comparable to pure PFO, while the 40% and 50% PVQ blend devices each showed a lower performance than the pure PFO device. Thus, enhancement of up to a factor of 5−14 is seen in the dilute PVQ blends (3−20%) compared to PFO homopolymer.

Similar relative enhancement in device performance was observed in the 5−20 wt % PS blends as shown in Figure 13. The best performance with a maximum brightness of 220 cd/m^2 and a maximum external efficiency of 0.10% at 13 V was found in the 10% PS blend.

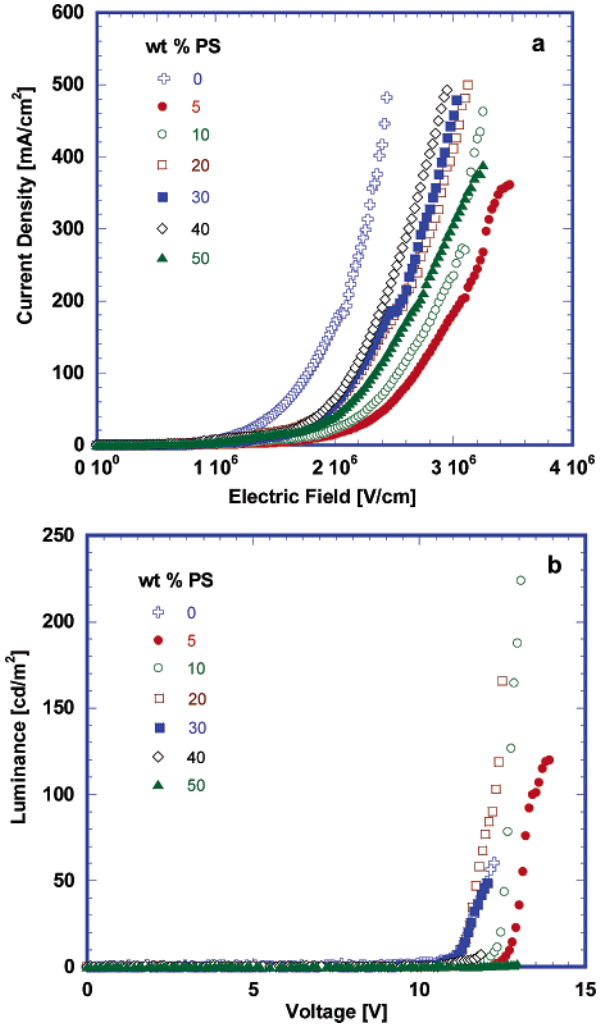

Figure 11. (a) Current density−electric field characteristics of LEDs: pure PFO and blends with PS. (b) Luminance−voltage characteristics of the devices in part a.

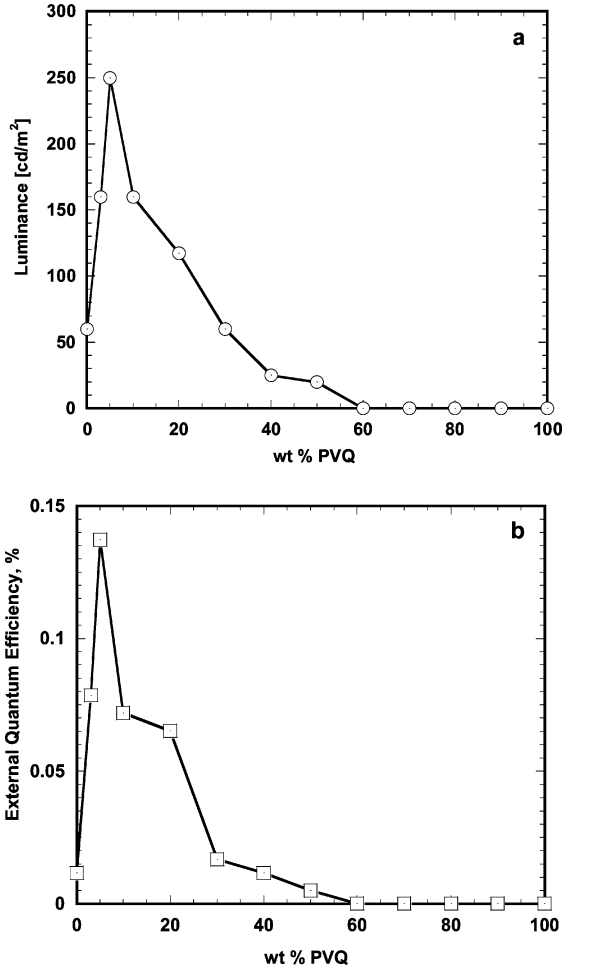

Figure 12. (a) Luminance and (b) external quantum efficiency of the PFO:PVQ blend LEDs as a function of blend composition.

This kind of enhancement in EL efficiency and brightness has been reported previously for several other polymer blend systems such as poly(2-methoxy-5-(2′-ethyl-hexyloxy)-1,4-phenylenevinylene) and poly(3-hexylthiophene) (MEHPPV:PHT),[17a] blends of polyquinolines,[17c] and binary blends of PFO.[17d,e] Maximum enhancement in device performance was observed in blends where the emissive component was the minor phase contrary to what is seen here in Figure 13.

Although the absolute brightness and efficiency of our devices are modest, we point out that all device fabrication and characterization were done in air. Almost all of the previous reports addressing EL stability of polyfluorene-based materials used Ca or Ca/Al cathodes, and the device characterizations were performed under inert atmosphere or in a vacuum.[6,7] This is a significant factor in light of the critical role of oxygen in accelerating the excimer formation in PFO.

Origin of EL Enhancement and Spectral Stability in PFO Blends. Previous reports on EL enhancement in polymer blends have attributed it to efficient energy transfer,[17a,b] exciton confinement,[17c,d] or improved charge carrier injection.[17e] In the present PFO blends, some energy transfer from the higher band gap PVQ to PFO is likely. However, the efficiency of energy transfer is expected to be very low due to insufficient overlap between the donor (PVQ) emission and acceptor (PFO) absorption (Figure 1a), the very low PL quantum yield of PVQ compared to PFO, and the morphology of the phase-separated blends. We think that in both blends, spatial confinement of excitons on the PFO chains is the primary reason for the observed factors of 5−14 enhancement in device brightness and efficiency. In the PFO:PVQ blends, PVQ serves more as a hole-blocking material than an electron-transporting one. There is no reduction in the turn-on voltage of the blend diodes with increasing PVQ content, suggesting that minority charge carrier (electron) injection is not much affected by the addition of PVQ. Also, since PVQ is a higher band gap material than PFO, the relative energy levels shown in Figure 1b suggest that both holes and electrons could be effectively trapped on PFO leading to better recombination efficiency. An enhanced electron−hole recombination efficiency can be concluded from the current−voltage characteristics of the diodes. Figure 10a clearly shows that the PVQ blend LEDs have lower currents than the PFO homopolymer devices by a factor of 8−10. However, due to the observed changes in the phase-separated morphology with varying blend composition, the effectiveness of the spatial confinement effects can be expected to vary with composition.

To investigate spatial confinement effects in the blends, we employed electric-field-modulated PL spectroscopy. PL quenching in conjugated polymers on application of electric fields is well-known to be due to exciton dissociation.[18] Figure 14 shows such PL spectra

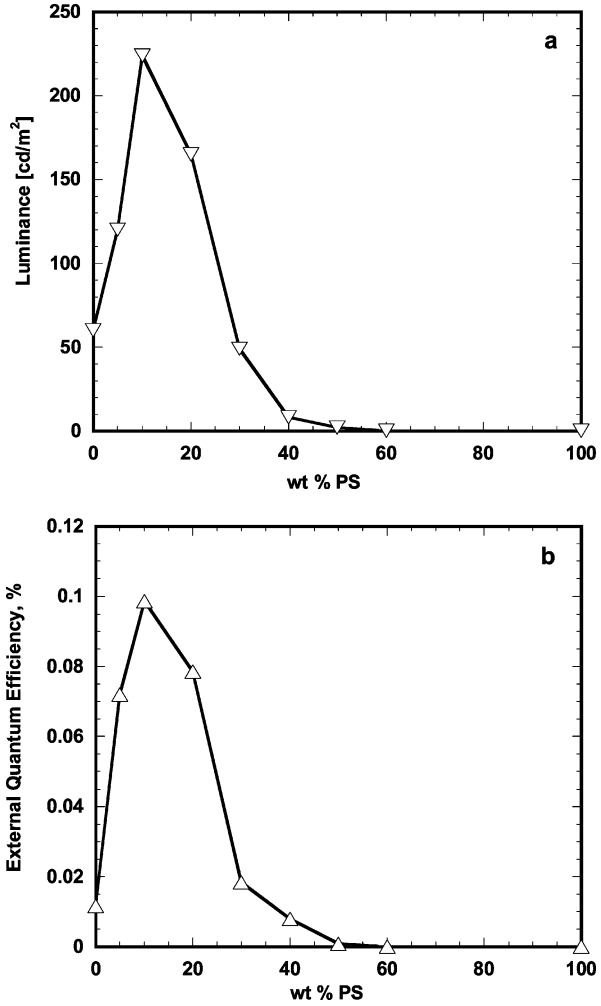

Figure 13. (a) Luminance and (b) external quantum efficiency of the PFO:PS blend LEDs as a function of blend composition.

for pure PFO and 5%, 10%, and 50% PVQ blends under different reverse bias voltages. It was confirmed from forward bias measurements before the EL turned on that only the electric field alters the PL spectra. The extent of PL quenching in pure PFO as seen in Figure 14a is much more than that for the 5% and 10% PVQ blends in Figure 14, parts b and c. The PL quenching in the 50% blend is relatively higher than that in the dilute blends.

Figure 15 depicts the relative PL efficiency for PFO and its blends with PVQ as a function of electric field. The relative PL efficiency is calculated as the ratio of the integrated PL intensity under application of electric field to that without the electric field. The pure PFO shows 40% quenching at a field of ~2.5 MV/cm, while the 5% PVQ blend shows only 5% quenching at the same operating field. Even at the high electric fields of ~4 MV/cm, where the peak brightness is seen in the blend LEDs, the PL is quenched by only 10% for the 3% and 5% PVQ blends. Thus, we can conclude that spatial confinement induced exciton stability occurs in all the blends compared to pure PFO.

We suggest that by acting as a hole blocking material, PVQ enhances the trapping of holes on the PFO polymer chains, thereby reducing their discharge at the cathode. Thus, the probability of these holes trapped on PFO to encounter an electron and form an exciton is improved in the blends, and hence giving the lower currents observed in the blend devices compared to the pure PFO diodes. In the case of PFO:PS blends, PS would have a similar hole and electron blocking effect in the blends due to its inert properties, resulting in lower currents in the corresponding devices. Such hole trapping is known to create a space charge near the anode and lead to a redistribution of the internal field which in turn helps the electron injection from the cathode.[19] All these results indicate that there is a better utilization of the majority carriers (holes) in the blends and that the excitons formed by the improved recombination efficiency are inherently more stable in the blends due to spatial confinement effects.

The observed lack of measurable EL in blends with a high concentration of PVQ (>50 wt %) is partly due to poor charge injection and transport. Exciton confinement effects shown to enhance device performance in the 3−20 wt % PVQ blends have largely disappeared at high concentrations of PVQ. From the PL quenching results in Figure 15, we note that as the fraction of PVQ increases from 3% to 50%, the degree of exciton stability is significantly decreased although still higher compared to PFO. These results can be understood in terms of the observed composition-dependent phase-separated morphology of the blends. We believe that the isolated islandlike domains of PFO seen in the morphology up to 30 wt % PVQ help to confining the excitons in the blends. Since the distance between the islands decreases in going from 3% to 30% PVQ, the extent of spatial confinement decreases. When the fraction of PVQ is 50% or higher in the blends, the topography smoothens dramatically (Figure 2) and the phase separation is not distinct, whereby excitons are no longer spatially confined in the PFO phase. Hence, the enhancement in EL efficiency is only seen in the 3−20 wt % PVQ composition with the maximum enhancement seen in the 5% PVQ blend.

The reason for the substantially better spectral stability in the PFO blend LEDs lies in the improved thermal resistance of the polymer blend films toward the heat developed during normal operation of the devices. As discussed earlier, a sharp increase in excimer emission at 530 nm was seen only on annealing the blend films at 200 °C. Since PVQ has a higher glass transition temperature (T_g) of 185 °C[8] compared to 75 °C[11a] for the pure PFO, the thermal resistance of the blends is better than the PFO homopolymer. Comparing the PFO blends with PVQ and PS, it is seen from Figures 8 and 9 that the PVQ blends exhibit better spectral stability. This is because the T_g of PS (101 °C) is much lower than that of PVQ (185 °C). It has also been observed that, for fluorene-based polymers, a higher glass transition temperature results in better thermal spectral stability and consequently better spectral stability in the EL.[6]

Conclusions

Spectrally stable blue electroluminescence is obtained from single-layer polymer light-emitting diodes (LEDs) made from binary blends of PFO with either poly(vinyl diphenylquinoline) or polystyrene. Enhanced performance was seen in terms of brightness and EL efficiency of the blend LEDs by a factor of 5−14 compared to PFO homopolymer devices. From the steady-state PL measurements, the electrical characteristics of the diodes, and electric-field-modulated PL spectroscopy studies, we infer that the EL enhancement results from spatial confinement induced exciton stability and improved

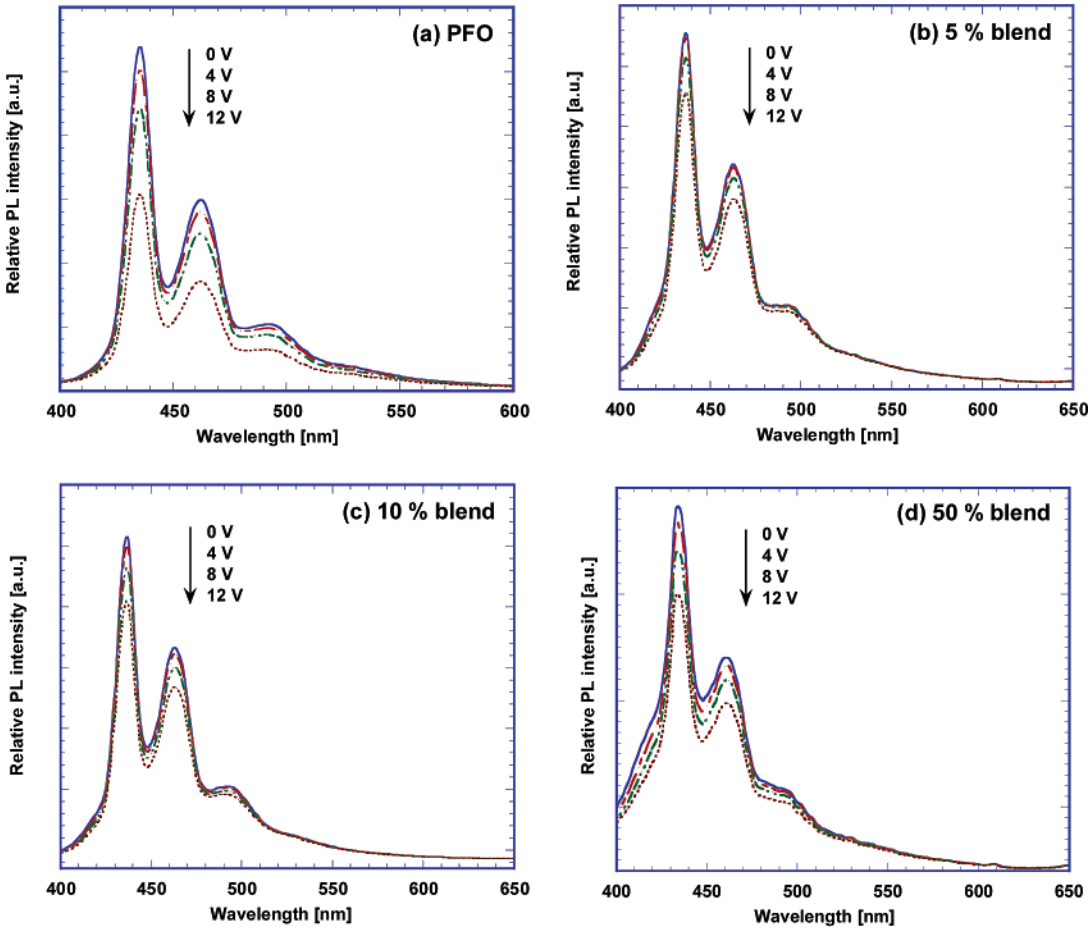

Figure 14. Electric-field-modulated PL emission spectra of (a) PFO, (b) 5% blend, (c) 10% blend, and (d) 50% PVQ blend. The excitation wavelength was 335 nm in all cases.

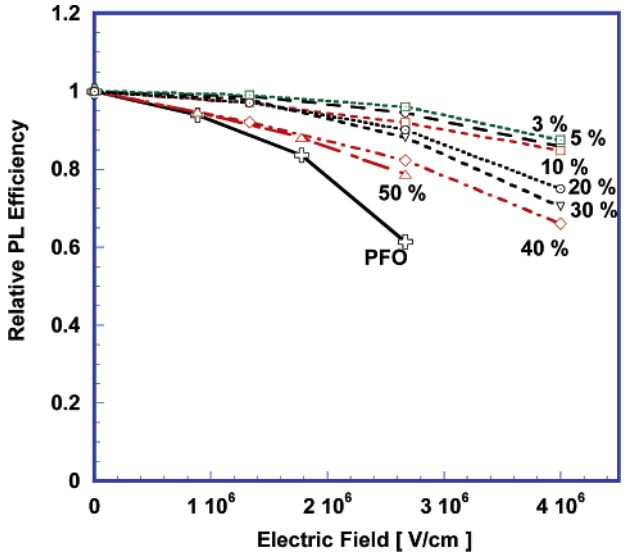

Figure 15. PL quenching as a function of electric field for PFO and its blends with PVQ.

electron−hole recombination efficiency. The variation in LED performance with blend composition was related to the phase-separated morphology of the blends. The improved EL spectral stability is due to the higher thermal stability of the blends on account of the higher T_g of both PVQ and PS relative to PFO. These results suggest that blending of blue-emitting polyfluorenes with a thermally stable charge transport/blocking polymer is a useful approach to realizing stable blue LEDs with enhanced performance and improved spectral characteristics.

Acknowledgment. This research was supported by the Army Research Office TOPS MURI (Grant DAAD19-01-1-0676) and in part by the Office of Naval Research.

References and Notes

(1) Recent reviews on polymer electroluminescence: (a) Friend, R. H.; Gymer, R. W.; Holmes, A. B.; Burroughes, J. H.; Marks, R. N.; Taliani, C.; Bradley, D. D. C.; Dos Santos, D. A.; Brédas, J. L.; Lögdlund, M.; Salaneck, W. R. *Nature (London)* **1999**, *397*, 121−128. (b) Bernius, M. T.; Inbasekaran, M.; O'Brien, J.; Wu, W. *Adv. Mater.* **2000**, *12*, 1737−1750. (c) Kraft, A.; Grimsdale, A. C.; Holmes, A. B. *Angew. Chem., Int. Ed.* **1998**, *37*, 402−428. (d) Heeger, A. J. *Solid State Commun.* **1998**, *107*, 673−679. (e) Kim, D. Y.; Cho, H. N.; Kim, C. Y. *Prog. Polym. Sci.* **2000**, *25*, 1089−1139.

(2) (a) Sokolik, I.; Yang, Z.; Karasz, F. E.; Morton, D. C. *J. Appl. Phys.* **1993**, *74*, 3584−3586. (b) Peng, Z.; Bao, Z.; Galvin, M. E. *Chem. Mater.* **1998**, *10*, 2086−2090. (c) Jenekhe, S. A.; Zhang, X.; Chen, X. L.; Choong, V.-E.; Gao, Y.; Hsieh, B. R. *Chem. Mater.* **1997**, *9*, 409−412. (d) Tarkka, R. M.; Zhang, X.; Jenekhe, S. A. *J. Am. Chem. Soc.* **1996**, *118*, 9438−9439. (e) Zhang, X.; Shetty, A. S.; Jenekhe, S. A. *Acta Polym.* **1998**, *49*, 52−55. (f) Zhang, X.; Shetty, A. S.; Jenekhe, S. A. *Macromolecules* **1999**, *32*, 7422−7429. (g) Zhang, X.; Jenekhe, S. A. *Macromolecules* **2000**, *33*, 2069−2082. (h) Alam, M. M.; Jenekhe, S. A. *Chem. Mater.* **2002**, *14*, 4775−4780. (i) Tonzola, C. J.; Alam, M. M.; Jenekhe, S. A. *Adv. Mater.* **2002**, *14*, 1086−1090.

(3) Recent reviews on polyfluorenes: (a) Neher, D. *Macromol. Rapid Commun.* **2001**, *22*, 1365−1385. (b) Scherf, U.; List, E. J. W. *Adv. Mater.* **2002**, *14*, 477−487. (c) Leclerc, M. *J. Polym. Sci., Part A: Polym. Chem.* **2001**, *39*, 2867−2873. (d) Becker, S.; Ego, C.; Grimsdale, A. C.; List, E. J. W.; Mar-

sitzky, D.; Pogantsch, A.; Setayesh, S.; Leising, G.; Mullen, K. *Synth. Met.* **2002**, *125*, 73−80.
(4) Redecker, M.; Bradley, D. D. C.; Inbasekaran, M.; Woo, E. P. *Appl. Phys. Lett.* **1998**, *73*, 1565−1567.
(5) (a) Bliznyuk, V. N.; Carter, S. A.; Scott, J. C.; Klärner, G.; Miller, R. D.; Miller, D. C. *Macromolecules* **1999**, *32*, 361−369. (b) List, E. J. W.; Guentner, R.; Scanducci de Freitas, P.; Scherf, U. *Adv. Mater.* **2002**, *14*, 374−378.
(6) (a) Yu, W.-L.; Pei, J.; Huang, W.; Heeger, A. J. *Adv. Mater.* **2000**, *12*, 828−831. (b) Zeng, G.; Yu, W.-L.; Chua, S.-J.; Huang, W. *Macromolecules* **2002**, *35*, 6907−6914. (c) Lee, J.-K.; Klarner, G.; Miller, R. D. *Chem. Mater.* **1999**, *11*, 1083−1088. (d) Kreyenschmidt, M.; Klaerner, G.; Fuhrer, T.; Ashenhurst, J.; Karg, S.; Chen, W. D.; Lee, V. Y.; Scott, J. C.; Miller, R. D. *Macromolecules* **1998**, *31*, 1099−1103. (e) Setayesh, S.; Grimsdale, A. C.; Weil, T.; Enkelmann, V.; Mullen, K.; Meghdadi, F.; List, E. J. W.; Leising, G. *J. Am. Chem. Soc.* **2001**, *123*, 946−953. (f) Wu, F.-I.; Reddy, D. S.; Shu, C.-F.; Liu, M. S.; Jen, A. K−Y. *Chem. Mater.* **2003**, *15*, 269−274. (g) Geng, Y. H.; Katsis, D.; Culligan, S. W.; Ou, J. J.; Chen, S. H.; Rothberg, L. J. *Chem. Mater.* **2002**, *14*, 463−470.
(7) (a) Sainova, D.; Miteva, T.; Nothofer, G.; Scherf, U.; Glowacki, I.; Ulanski, J.; Fujikawa, H.; Neher, D. *Appl. Phys. Lett.* **2000**, *76*, 1810−1812. (b) Grice, A. W.; Bradley, D. D. C.; Bernius, M. T.; Inbasekaran, M.; Wu, W. W.; Woo, E. P. *Appl. Phys. Lett.* **1998**, *73*, 629−631. (c) Weinfurtner, K.-H.; Fujikawa, H.; Tokito, S.; Taga, Y. *Appl. Phys. Lett.* **2000**, *76*, 2502−2504. (d) Palilis, L. C.; Lidzey, D. G.; Redecker, M.; Bradley, D. D. C.; Inbasekaran, M.; Woo, E. P.; Wu, W. W. *Synth. Met.* **2001**, *121*, 1729−1730.
(8) Lu, L.; Jenekhe, S. A. *Macromolecules* **2001**, *34*, 6249−6254.
(9) The external quantum efficiency is calculated using

$$\phi_{EL} = \frac{\pi e}{K_m hc}\frac{L}{J}\left[\frac{\int F(\lambda)\,d\lambda}{\int (1/\lambda)F(\lambda)y(\lambda)\,d\lambda}\right]$$

where L is the luminance (cd/m^2) of the device at a current density of J (A/m^2), K_m is a conversion constant based on the maximum sensitivity of the eye (680 lm/W), $y(\lambda)$ is the normalized photopic spectral response function, $F(\lambda)$ is the EL spectrum, and λ is the wavelength.
(10) (a) Liao, L. S.; Fung, M. K.; Lee, C. S.; Lee, S. T.; Inbasekaran, M.; Woo, E. P.; Wu, W. W. *Appl. Phys. Lett.* **2000**, *76*, 3582−3584. (b) Janietz, S.; Bradley, D. D. C.; Grell, M.; Giebler, C.; Inbasekaran, M.; Woo, E. P. *Appl. Phys. Lett.* **1998**, *73*, 2453−2455.
(11) (a) Grell, M.; Bradley, D. D. C.; Ungar, G.; Hill, J.; Whitehead, K. S. *Macromolecules* **1999**, *32*, 5810−5817. (b) Grell, M.; Bradley, D. D. C.; Inbasekaran, M.; Woo, E. P. *Adv. Mater.* **1997**, *9*, 798−802. (c) Grell, M.; Bradley, D. D. C.; Long, X.; Chamberlain, T.; Inbasekaran, M.; Woo, E. P.; Soliman, M. *Acta Polym.* **1998**, *49*, 439−444. (d) Bradley, D. D. C.; Grell, M.; Long, X.; Mellor, H.; Grice, A.; Inbasekaran, M.; Woo, E. P. *Proc. SPIE* **1997**, *3145*, 254−259.
(12) (a) Agrawal, A. K.; Jenekhe, S. A. *Macromolecules* **1993**, *26*, 895−905. (b) Agrawal, A. K.; Jenekhe, S. A. *Chem. Mater.* **1996**, *8*, 579−589.
(13) Paul, D. R.; Bucknall, C. B., Eds. *Polymer Blends*; John Wiley & Sons: New York, 2000.
(14) (a) Arias, A. C.; MacKenzie, J. D.; Stevenson, R.; Halls, J. J. M.; Inbasekaran, M.; Woo, E. P.; Richards, D.; Friend, R. H. *Macromolecules* **2001**, *34*, 6005−6013. (b) Babel, A.; Jenekhe, S. A. *J. Phys. Chem. B* **2002**, *106*, 6129−6132. (c) Babel, A.; Jenekhe, S. A. *J. Phys. Chem. B* **2003**, *107*, 1749−1754.
(15) (a) Jenekhe, S. A.; Osaheni, J. A. *Science* **1994**, *265*, 765−768. (b) Jenekhe, S. A. *Adv. Mater.* **1995**, *7*, 309−311. (c) Osaheni, J. A.; Jenekhe, S. A. *Macromolecules* **1994**, *27*, 739−742.
(16) (a) Teetsov, J.; Bout, D. A. V. *Langmuir* **2002**, *18*, 897−903. (b) Lee, J.-I.; Klaerner, G.; Miller, R. D. *Synth. Met.* **1999**, *101*, 126. (c) Teetsov, J.; Fox, M. A. *J. Mater. Chem.* **1999**, *9*, 2117−2122.
(17) (a) Yu, G.; Nishino, H.; Heeger, A. J.; Chen, T.-A.; Rieke, R. D. *Synth. Met.* **1995**, *72*, 249−252. (b) Lee, J.-I.; Kang, I.-N.; Hwang, D.-H.; Shim, H.-K.; Jeoung, S. C.; Kim, D. *Chem. Mater.* **1996**, *8*, 1925−1929. (c) Zhang, X.; Kale, D. M.; Jenekhe, S. A. *Macromolecules* **2002**, *35*, 382−393. (d) Charas, A.; Morgado, J.; Martinho, J. M. G.; Fedorov, A.; Alcacer, L.; Cacialli, F. *J. Mater. Chem.* **2002**, *12*, 3523−3527. (e) Campbell, A. J.; Antoniadis, H.; Virgili, T.; Lidzey, D. G.; Wang, X.; Bradley, D. D. C. *Proc. SPIE* **2002**, *4464*, 211−222.
(18) (a) Chen, X. L.; Jenekhe, S. A. *Appl. Phys. Lett.* **1997**, *70*, 487−489. (b) Chen, X. L.; Jenekhe, S. A. *Macromolecules* **1996**, *29*, 6189−6192. (c) Deussen, M.; Scheidler, M.; Bassler, H. *Synth. Met.* **1995**, *73*, 123−129.
(19) (a) Campbell, A. J.; Bradley, D. D. C.; Antoniadis, H. *J. Appl. Phys.* **2001**, *89*, 3343−3351. (b) Malliaras, G. G.; Scott, J. C. *J. Appl. Phys.* **1998**, *83*, 5399−5403.

MA0344700